A C-Terminal Dimerization Motif Is Required for Focal Adhesion Targeting of Talin1 and the Interaction of the Talin1 I/LWEQ Module with F-Actin†

Steven J. Smith and Richard O. McCann*

Department of Molecular and Cellular Biochemistry, College of Medicine, University of Kentucky, 741 South Limestone Street, Lexington, Kentucky 40536-0509

Received April 3, 2007; Revised Manuscript Received June 5, 2007

ABSTRACT: Focal adhesion complexes are plasma membrane-associated multicomponent complexes that are essential for integrin-linked signal transduction as well as cell adhesion and cell motility. The cytoskeletal protein Talin1 links integrin adhesion receptors with the actin cytoskeleton. Talin1 and the other animal and amoebozoan talins are members of the I/LWEQ module superfamily, which also includes fungal Sla2 and animal Hip1/Hip1R. The I/LWEQ module is a conserved C-terminal structural element that is critical for I/LWEQ module protein function. The I/LWEQ module of Talin1 binds to F-actin and targets the protein to focal adhesions in vivo. The I/LWEQ modules of Sla2 and Hip1 are required for the participation of these proteins in endocytosis. In addition to these roles in I/LWEQ module protein function, we have recently shown that the I/LWEQ module also contains a determinant for protein dimerization. Taken together, these results suggest that actin binding, subcellular targeting, and dimerization are associated in I/LWEQ module proteins. In this report we have used alanine-scanning mutagenesis of a putative coiled coil at the C-terminus of the Talin1 I/LWEQ module to show that the amino acids responsible for dimerization are necessary for F-actin binding, the stabilization of actin filaments, the cross-linking of actin filaments, and focal adhesion targeting. Our results suggest that this conserved dimerization motif in the I/LWEQ module plays an essential role in the function of Talin1 as a component of focal adhesions and, by extension, the other I/LWEQ module proteins in other multicomponent assemblies involved in cell adhesion and vesicle trafficking.

Focal adhesion complexes are multicomponent plasma membrane-associated protein assemblies that are essential for integrin-linked signal transduction and for cell adhesion and cell motility (*1*, *2*). In focal adhesions, heterodimeric α/*β*-integrins interact simultaneously with components of the extracellular matrix (ECM)[1] such as fibronectin and collagen and intracellular cytoskeletal proteins such as Talin1 to complete the linkage between the ECM and the actin cytoskeleton. Multiple protein−protein interactions between additional focal adhesion components such as vinculin, paxillin, focal adhesion kinase (FAK), zyxin, and α-actinin mediate focal adhesion functions. As a primary link between the cytoplasmic tail of *β*-integrin and the actin cytoskeleton (*3*−*5*), Talin1 is essential for the assembly of focal adhesions (*6*) and is also a physiological partner of a number of other focal adhesion proteins. The N-terminal FERM domain (*7*) of Talin1 interacts with integrin, FAK, PIPKIγ, actin, and layilin (*8*−*13*), and the central α-helical rod domain contains binding sites for vinculin, integrin, actin, and TES (*12*, *14*−*16*). The C-terminal I/LWEQ module of Talin1 interacts with F-actin (*17*−*19*) and also targets Talin1 to focal adhesions (*20*).

The I/LWEQ module has a consensus length of 186 amino acids and defines a superfamily of actin-binding proteins that includes the animal and amoebozoan talins, fungal Sla2, and the animal and amoebozoan Hip1 and Hip1R, which are homologues of Sla2 (*17*). The conserved structural organization of I/LWEQ module proteins allows these proteins to serve as linkers to the actin cytoskeleton in diverse cellular processes (*17*, *19*, *21*). These proteins have a similar modular organization with a C-terminal I/LWEQ module, a central α-helical domain, and either an N-terminal FERM domain for talins or an N-terminal ANTH domain for Sla2/Hip1 (*17*, *18*). The FERM domain targets proteins to the inner face of the plasma membrane (*7*), while the ANTH domain (AP-180 N-terminal homology) is a PtdIns(4,5)P_2-binding element found in proteins involved in receptor-mediated endocytosis (*22*). Consistent with its evolutionary conservation, the I/LWEQ module is essential for the function of these proteins. The I/LWEQ module of *Schizosaccharomyces pombe* Sla2p is necessary for the establishment of a new growth zone and polarization of the actin cytoskeleton during cell division (*23*). In *Saccharomyces cerevisiae* Sla2p is required for the internalization step of endocytosis; this requires the I/LWEQ module, which suggests that the

† This work was supported by grants from the American Cancer Society (85-001-13-IRG) and the National Institutes of Health (P20RR20171) to R.O.M. S.J.S. is supported by a Research Challenge Trust Fund Fellowship from the University of Kentucky.

* Corresponding author. E-mail: rmcca1@uky.edu. Phone: 859-323-1796. Fax: 859-323-1037.

[1] Abbreviations: DTSSP, 3,3′-dithiobis(sulfosuccinimidyl) propionate; DTT, dithiothreitol; ECM, extracellular matrix; FAK, focal adhesion kinase; PtdIns(4,5)P_2, phosphatidylinositol 4,5-bisphosphate; PIPKIγ, type I phosphatidylinositol phosphate kinase isoform γ; SDS−PAGE, sodium dodecyl sulfate−polyacrylamide gel electrophoresis; K_d, dissociation constant; B_{max}, maximal binding; EDTA, ethylenediaminetetraacetic acid; PBS, phosphate-buffered saline.

10.1021/bi700637a CCC: $37.00
Published on Web 08/28/2007

I/LWEQ module stabilizes actin as it assembles with the endocytic vesicles (*24*, *25*). Similarly, in animal cells clathrin-coated cargo accumulates near the plasma membrane when a truncated Hip1R mutant lacking the I/LWEQ module is overexpressed in mammalian cells (*26*). The Talin1 I/LWEQ module is required for the force transduction linkage between the actin cytoskeleton and the ECM in mammalian cells. The two piconewton slip bond between a fibronectin-coated bead, which is a proxy for the ECM, and the actin cytoskeleton is absent in Talin1-*null* cells (*27*). This linkage could be restored by expression of exogenous full-length Talin1, but Talin1 lacking the I/LWEQ module was unable to rescue the mutant phenotype. Furthermore, Talin1-*null* cells expressing truncated Talin1 without the I/LWEQ module failed to assemble focal adhesions (*28*). Consistent with these results, we have recently shown that the Talin1 constructs containing binding sites for focal adhesion components such as vinculin, FAK, and integrin, but lacking the I/LWEQ module, did not target to focal adhesions. The I/LWEQ module alone is both necessary and sufficient for targeting Talin1 to focal adhesions, and this subcellular targeting is largely separable from actin binding (*20*).

The I/LWEQ modules of all superfamily members share a similar structural organization consisting of five α-helices connected by short loop regions (*17*, *18*). We previously used an in silico approach to predict that the I/LWEQ module of Talin1 forms a five-helix bundle (*19*) and have shown using circular dichroism that the consensus sequence is >90% α-helical (*20*). More recently, a crystal structure of the C-terminus of Hip1R confirmed that the I/LWEQ module plus the upstream α-helix (*29*), which is not part of the I/LWEQ module proper, exists as a five-helix bundle. However, that structure lacks the final α-helix (block 4), which we have shown previously (*17*, *20*) and in this report to be important for I/LWEQ module function. Previous studies have indicated that Talin1 is a dimer in vivo (*30*), but the exact mechanism responsible for this dimerization is not well characterized. We have previously shown that the I/LWEQ modules of Talin1 and *Dictyostelium discoideum* TalA exist as dimers in solution (*19*). Brett et al. also have proposed that oligomerization is critical to Hip1R I/LWEQ module function (*29*). In the present study we have shown that the final α-helix of the Talin1 I/LWEQ module contains this dimerization determinant. This part of Talin1 is also essential for actin binding and focal adhesion targeting (*20*). The close apposition of dimerization with actin binding and subcellular targeting signals in Talin1 suggests that dimerization is associated with these essential functions of Talin1. Projection of the final α-helix of Talin1 onto a helical wheel diagram revealed a possible mechanism for dimerization. The eight most conserved residues are on one face of the α-helix, in an alternating pattern of hydrophobic and charged residues that are predicted to form a coiled coil (*31*). Given that coiled coils are common dimerization motifs in proteins, this region of the I/LWEQ module could be responsible for dimerization.

To test this hypothesis we performed alanine-scanning mutagenesis on these conserved amino acids. We found that mutation of the core residues, as both single and multiple mutations involving the hydrophobic and charged residues, lessened the dimeric character while simultaneously decreasing the actin-binding capacity of the Talin1 I/LWEQ module. These mutants also showed defects in the bundling, cross-linking, and stabilization of actin filaments. Furthermore, several of these mutations also reduced or abolished focal adhesion targeting. Each of these properties of the I/LWEQ module are likely to be important for the function of Talin1 as a component of dynamic focal adhesions (*32*). Our results have identified additional activities of Talin1 that are mediated by the conserved I/LWEQ module and indicate that dimerization is likely to be essential for Talin1 function. Further work on these mutations in the context of the full-length protein will identify the precise cellular roles of these properties of Talin1 in focal adhesion dynamics, cell adhesion and motility, and focal adhesion-linked signaling. Given the evolutionary conservation of this region, our results will also provide a foundation for studying how dimerization, actin binding, and perhaps subcellular targeting of Sla2p/Hip1 are integrated in endocytosis, cell division, and the establishment of cell polarity.

EXPERIMENTAL PROCEDURES

Expression Plasmid Constructs. MmTalin1.2345-2541 (I/LWEQ module) has been described previously (*19*). Using that construct as the wild-type foundation, we prepared the following I/LWEQ module mutants using the QuikChange (Stratagene) site-directed mutagenesis protocol: Q2505A (Q1A); L2509A (L2A); E2512A (E3A); L2515A (L4A); R2519A (R5A); L2522A (L6A); R2526A (R7A); Y2530A (Y8A); L2509A + L2515A (L24A); L2509A + L2522A (L26A); L2515A + L2522A (L46A); E2512A + R2519A (E3R5A); and L2509A + L2515A + L2522A (L246A). The following sense with cognate antisense (not shown) oligonucleotides (Integrated DNA Technologies) were used in mutagenesis: Q1A, 5′-CAGATTATCGCAGCAGCGGAAGAGATGCTTCGG-3′; L2A, 5′-GCACAGGAAGAGATGGCACGGAAGGAACGAGAG-3′; E3A, 5′-GAGATGCTTCGGAAGGCACGAGAGCTGGAAGAG-3′; L4A, 5′-CTTCGGAAGGAACGAGAGGCGGAAGAGGCTCGGAAAAAG-3′; R5A, 5′-CTGGAAGAGGCTGCGAAAAAGCTCGCC-3′; L6A, 5′-GCTGCGAAAAAGGCCGCCCAGATCCGG-3′; R7A, 5′-GTCTAGGCCCAGATCGCGCAGTACAAGTTC-3′; Y8A, 5′-CAGATCCGGCAGCAGCAGGCCAAGTTCTTGCCTTCAGAG-3′.

Double and triple mutations were constructed using a previously generated mutant and the appropriate oligonucleotides for the second and third mutations. Mutant GFP-fusion constructs were prepared by subcloning the coding sequences into pEGFP-C3 (Clontech). The DNA sequence of each construct was verified independently by DNA sequence determination.

Protein Preparation. 6His-fusion proteins were purified using immobilized metal affinity chromatography (IMAC) as described previously (*19*). Following cleavage of the 6His tag proteins were further purified by size exclusion chromatography using Sephacryl 100-HR. Protein purity and 6His tag cleavage were confirmed using SDS−PAGE.

F-Actin Binding. I/LWEQ module protein solutions were precleared by centrifugation at 160000*g* for 20 min to remove potential protein aggregates prior to protein concentration determination using the calculated extinction coefficient. F-Actin cosedimentation assays were then performed as previously described (*19*). The binding data (three or four

for independent replicates for each assay) were then plotted using GraphPad Prism 4.0 and fit to a rectangular hyperbola for calculation of binding constants and maximal binding values ($Y = B_{max}X/K_d + X$; B_{max} = maximal binding; K_d = dissociation constant). The recombinant wild-type and mutant proteins did not sediment in the absence of F-actin. F-Actin bands serving as internal controls confirmed an accurate linearity of response for densitometry measurements.

Gel Filtration Chromatography. Standards and Talin1 I/LWEQ module proteins were chromatographed on Sephacryl S100-HR (1.5 cm × 50 cm) in 10 mM Tris, pH 8.0, 25 mM KCl, 1 mM EDTA, and 0.02% sodium azide at a flow rate of 0.3 mL min^{-1}. The column was calibrated with the following standards (Sigma): blue dextran (2000 kDa), bovine serum albumin (67 kDa), ovalbumin (45 kDa), carbonic anhydrase (31 kDa), and cytochrome *c* (12.7 kDa). Identification of the I/LWEQ module proteins in the elution fractions was determined using absorbance at 280 nm and confirmed by SDS−PAGE gel electrophoresis coupled with silver staining.

Chemical Cross-Linking. 3,3′-Dithiobis(sulfosuccinimidyl) propionate (DTSSP; Pierce), which is a reversible chemical cross-linker, was used to identify I/LWEQ module dimers in solution. Wild-type and mutant I/LWEQ module protein solutions (35 μM) were incubated with excess DTSSP (0.5 mM) in PBS (25 mM sodium phosphate, 150 mM NaCl, pH 7.2) at 22 °C for 30 min. The cross-linking reactions were then quenched with 50 mM Tris, pH 7.5, for 15 min. The reaction mixture was split into two fractions, and each half was analyzed using SDS−PAGE under either reducing (50 mM DTT) or nonreducing denaturing conditions to identify reversibly cross-linked species. These were visualized by immunoblotting with antibodies to the T7 tag (Novagen) in the cleaved 6His protein or Talin1-specific antibodies (*21*).

F-Actin Stabilization. F-Actin depolymerization was measured in the presence of Talin1 I/LWEQ module proteins using a fluorescence assay (*33*). Complete polymerization of 10 μM pyrene−actin (Cytoskeleton, Inc.) was monitored by the increase in pyrene fluorescence at 407 nm (excitation at 365 nm), which reached a maximum in 30 min and remained stable during the course of each experiment. The polymerized F-actin was then diluted 100-fold to a final concentration of 0.1 μM in buffer A in a total volume of 500 μL to induce depolymerization. The dilution buffer contained the Talin1 I/LWEQ module protein being assayed at a final concentration of 1.0 μM. Actin depolymerization was monitored by the decrease in fluorescence using a Perkin-Elmer Model LS55 luminescence spectrometer. Depolymerization was followed for 10 min at 22 °C, and the data were plotted using Graph Prism 4.0. The resulting curves are the averages of three to five independent assays. The data were normalized using the F-actin stabilization activity of the wild-type protein as 100% and the actin-only or actin-GST (1.0 μM) controls as 0% stabilization activity.

Actin Cross-Linking by Talin1 I/LWEQ Module Proteins. Actin cross-linking by the Talin1 I/LWEQ module proteins was measured using low-speed centrifugation. Actin (3.0 μM) was polymerized in the presence of the I/LWEQ module protein (3.0 μM) in a total volume of 50 μL for 60 min at 22 °C. The reaction was then centrifuged for 20 min at 13000*g*. Following SDS−PAGE, proteins in the supernatant and pellet fractions were stained using Coomassie Blue G250, and the amount of the I/LWEQ module in each fraction was quantified densitometrically using NIH image v1.62. Normalized results, with the wild-type Talin1 I/LWEQ module as 100% cross-linking activity, from four to five independent assays were then plotted using GraphPad Prism 4.0.

Electron Microscopy. Actin (3.0 μM) was polymerized in the presence of the I/LWEQ module protein (3.0 μM) in a total volume of 50 μL for 60 min at 22 °C. The F-actin was then incubated on a Formvar carbon-coated grid (Electron Microscopy Sciences) for 90 s. After excess liquid was removed by blotting with filter paper, the grid was stained with 2% uranyl acetate (Electron Microscopy Sciences) for 60 s. The grids were then air-dried for 2 h. Electron micrographs were obtained at 83000× magnification using a Philips Technai transmission electron microscope, and digital images were acquired using Gatan software.

Cell Culture, Transfections, and Fluorescence Microscopy. HeLa cells were cultured on fibronectin at a density of 15000 cells per coverslip as previously described (*20*) and incubated for 24 h. The cells were then transfected with each GFP-Talin1 I/LWEQ module construct using FuGENE 6.0. After incubation for 24 h, the transfected cells were fixed in fresh 4% paraformaldehyde in PBS for 20 min at 4 °C and then permeabilized with 1% Triton X-100 in PBS for 20 min at 0 °C. The fixed, permeabilized cells were then blocked with 1% normal goat serum in PBS for 1 h at 4 °C and incubated overnight with anti-vinculin (Sigma V-9131, 1:400 dilution) in 1% normal goat serum/PBS. The cells were then washed with PBS and incubated with a goat anti-mouse rhoadmine-labeled secondary antibody for 1 h at 4 °C in a humidified chamber. The coverslips were mounted using VectaShield (containing DAPI), and fluorescent images were obtained using a Nikon Eclipse TE600 microscope. Digital images were acquired using MetaMorph (Molecular Devices). The expression of each intact GFP-I/LWEQ module fusion construct was verified by immunoblotting of transfected cultures using anti-GFP.

RESULTS

The C-Terminal Block 4 of the I/LWEQ Module of Talin1 Contains a Dimerization Motif. It has been reported previously that full-length Talin1 is isolated as a dimer and functions as a dimer in vivo (*30*). We previously showed that the Talin1 I/LWEQ module exists as a dimer in solution (*19*). Using both gel filtration and chemical cross-linking, we have determined here that dimerization requires the C-terminal block 4 of the I/LWEQ module. As with the full-length protein and the I/LWEQ module, each of the I/LWEQ module truncation mutants containing block 4 (T1−T4) behaved as a dimer during gel filtration and chemical cross-linking using DTSSP (Figure 1A). Interestingly, comparison of these results with our previous analysis of the I/LWEQ module (*19*) shows that dimerization of these I/LWEQ module proteins also correlates with actin binding and focal adhesion targeting of the Talin1 I/LWEQ module. Only truncations which contain block 4 are dimers in solution, bind to F-actin, and localize to focal adhesions (Figure 1A). None of the truncations (T5−T8) which lack block 4 dimerizes, binds to F-actin, or is targeted to focal adhesions. These results suggest that the I/LWEQ module must be a

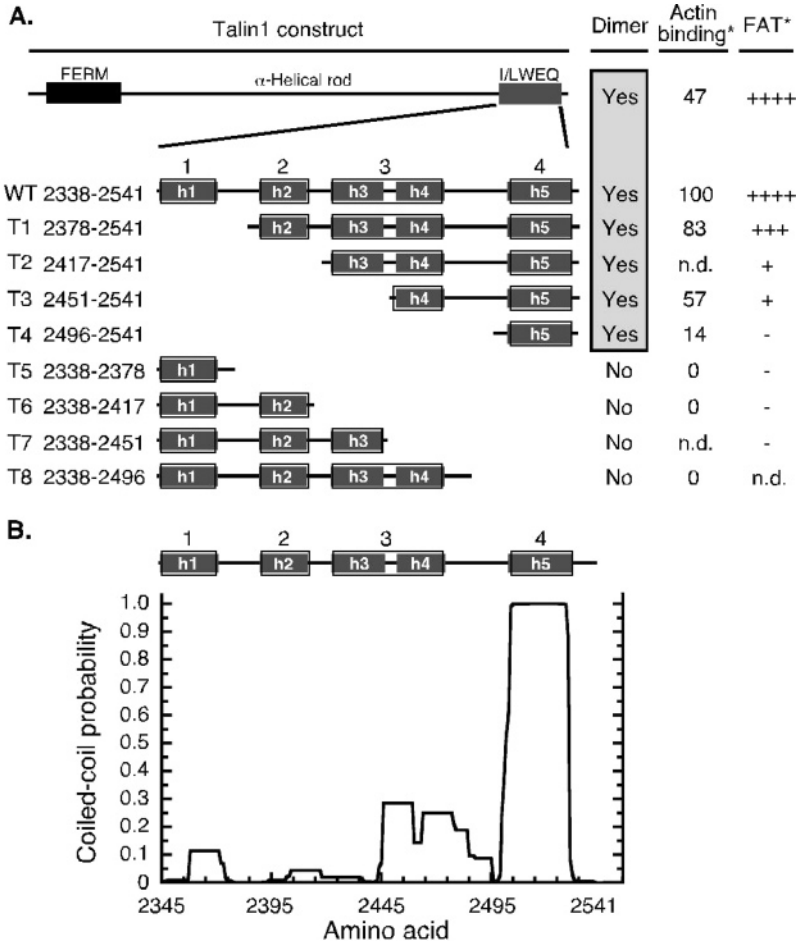

FIGURE 1: Identification of the dimerization signal in block 4 of the Talin1 I/LWEQ module. (A) Truncation mutagenesis showed that block 4 is essential for dimerization of the Talin1 I/LWEQ module. Only constructs containing block 4/helix 5 behaved as dimers, as assayed by gel filtration and chemical cross-linking. Columns marked with asterisks indicate that block 4 is also required for actin binding and focal adhesion targeting (FAT), as we have shown previously (*20*). (B) Analysis of the Talin1 I/LWEQ module using Coils (*31*) predicted that the block 4/helix 5 sequence is very likely to form a coiled coil, which could account for the dimerization of the constructs containing block 4.

dimer to perform several of its critical functions as a structural element of Talin1 and that the α-helix (helix 5) coextensive with block 4 is the likely dimerization determinant.

To identify potential mechanisms that could account for dimerization of block 4, we performed several secondary structure predictions on the I/LWEQ module, in addition to that shown in Figure 1A, which is a recapitulation of our previous results showing that the I/LWEQ module is a highly α-helical structural element probably consisting of a five-helix bundle (*19*). The analysis in Figure 1B using the Coils prediction algorithm shows that block 4 has a very high probability of forming a coiled coil (*31*); other algorithims, such as Paircoil (*34*), produced a similar result (not shown). Coiled coil motifs can be stabilized by interactions between both hydrophobic and charged amino acids, which result in proper alignment, orientation, and selectivity of the coiled coil (*35*). A closer examination of the block 4 sequence revealed that eight of the amino acids of block 4 are nearly universally conserved among all members of the I/LWEQ module superfamily (Figure 2A, residues 1−8). Consistent with the hypothesis that block 4 forms a coiled coil, we also found that when the block 4 α-helix is projected onto a helical wheel, all eight residues lie on the same face of the α-helix (Figure 2B). Thus, a coiled coil could form between adjacent block 4 α-helices, with hydrophobic interactions between the leucine residues (L2−L6, L4−L4, and L6−L2) and electrostatic interactions by the charged residues (E3−R5 and R5−E3). This coiled coil would likely be antiparallel; similar coiled coils have been identified in previously characterized proteins (*36*). To determine whether these amino acids mediate dimerization of the Talin1 I/LWEQ module, we performed an alanine-scanning mutagenesis of residues Q1A, L2A, E3A, L4A, R5A, L6A, R7A, and Y8A and multiple mutants of the internal hydrophobic and charged residues (L24A, L26A, L46A, L246A, E3R5A).

Dimerization of the Talin1 I/LWEQ Module Is Mediated by the Conserved Face of Block 4. We used gel filtration and chemical cross-linking of the alanine mutants to determine whether the conserved amino acids of block 4 mediate I/LWEQ module dimerization. As expected based on our previous study of the I/LWEQ module (monomer molecular mass: 23 kDa), gel filtration confirmed that the wild-type protein behaves as a dimer in solution, by coeluting with ovalbumin, which has a molecular mass of 45 kDa (Figure 3A). In contrast to the unmodified protein, each of the mutants, except for Y8A, eluted from the same column with an apparent molecular mass of approximately 35−36 kDa, which is intermediate between the calculated monomer and dimer molecular masses and is indicative of a monomer−

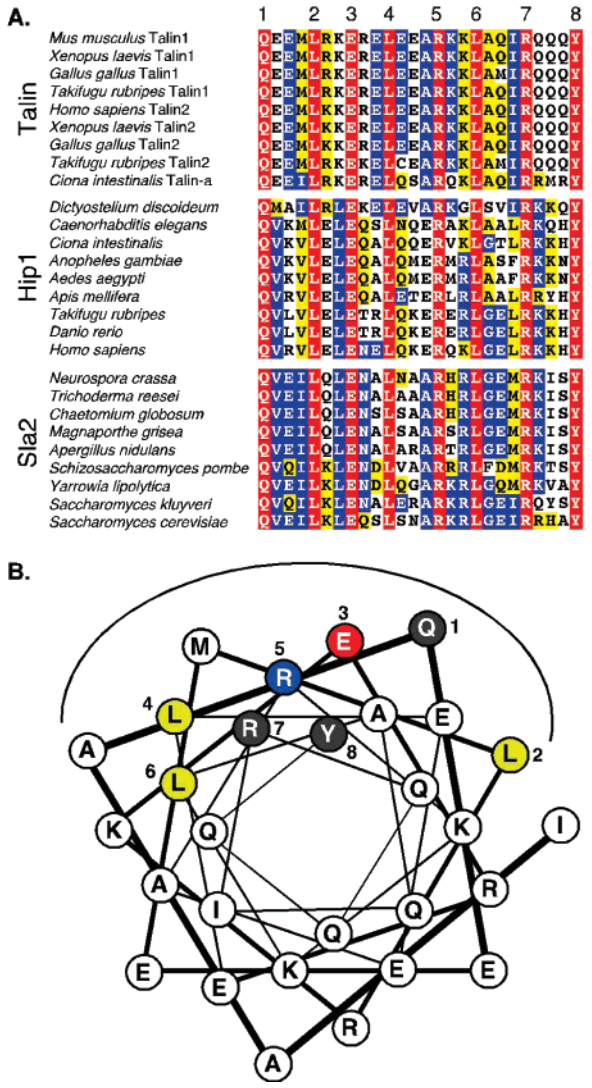

FIGURE 2: Sequence conservation of block 4 of the I/LWEQ module. (A) Amino acid sequence alignment of block 4 of representatives of the I/LWEQ module superfamily, including animal talin, animal Hip1, and fungal Sla2. The most conserved residues 1−8 have been subjected to alanine-scanning mutagenesis in this report. Key: red, identities; blue, conserved amino acids; yellow, similar amino acids. (B) Projection of the block 4 α-helix onto a helical wheel diagram shows that amino acids 1−8 lie on one face of the helix (arc). The conserved leucines (2, 4, and 6) are in yellow; the internal charged residues (E3, R5) are in red and blue, respectively; Q1, R7, and Y8, which are outside of the core of the putative coiled coil, are in gray.

dimer equilibrium. The double and triple leucine mutants (L24A, L26A, L46A, and L246A) and the double E3R5A mutant also eluted as monomer−dimer mixtures. The Y8A mutant eluted with an apparent molecular mass of 45 kDa, which is consistent with a dimer for this protein. These data (Figure 3A) suggest that the mutations disrupted the stability of the dimerization motif associated with the putative coiled coil region of block 4 and prevented the Talin1 I/LWEQ module from forming a stable dimer in solution.

We further analyzed the strength of these dimers using chemical cross-linking. Wild-type and mutant Talin1 I/LWEQ module proteins were treated with the homobifunctional amine-reactive, cleavable cross-linker DTSSP, and cross-linked species were identified using SDS−PAGE. These results are shown in Figure 3B. In the absence of cross-linker, under denaturing conditions most of the wild-type Talin1

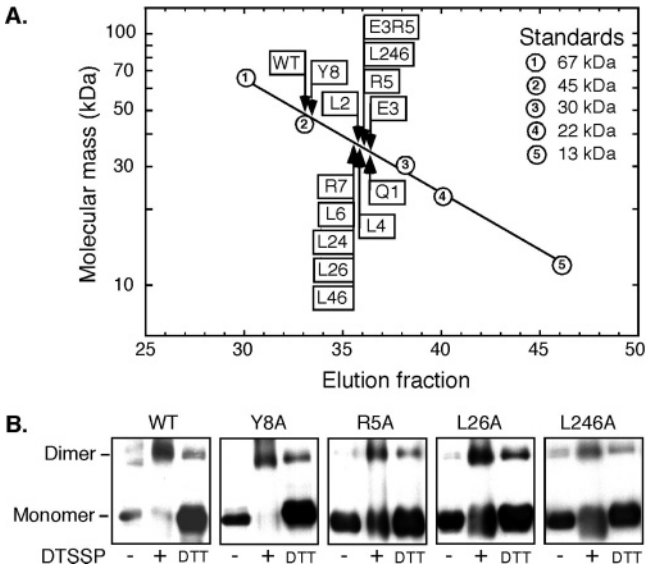

FIGURE 3: Talin1 I/LWEQ module dimerization. (A) Gel filtration chromatography showed that the wild-type I/LWEQ module and the Y8A mutant elute as a dimer, while each of the other mutants eluted as an apparent monomer−dimer mix. (B) Chemical cross-linking confirmed the gel filtration results. Treatment of the dimeric WT and Y8A with DTSSP converted nearly all of the protein to a dimeric species (middle lane) under nonreducing denaturing conditions, which could be subsequently converted back into a monomer under reducing conditions (right lane). Conversion of the monomeric mutants (R5A, L26A, and L246A) into dimers was less efficient (middle lane) under identical cross-linking conditions. Similar results were obtained with the other monomeric mutants (not shown).

I/LWEQ module existed as a monomer (panel 1, left lane). Treatment of this protein with DTSSP converted the bulk of the protein to the dimeric species (panel 1, lane 2; denaturing, nonreducing conditions). Treatment of the cross-linked species with the reducing agent dithiothreitol converted the protein back into a predominantly monomeric species (panel 1, lane 3; denaturing and reducing conditions). We obtained similar results with the Y8A mutant (panel 2), which is also a predominantly dimeric protein according to gel filtration (Figure 3A). Representative cross-linking results for single (R5A), double (L26A), and triple (L246A) mutants are shown in panels 3−5, respectively. With each of these mutants, chemical cross-linking was much less efficient than with the wild-type and Y8A proteins, which is demonstrated by the increased amount of un-cross-linked protein in each center lane. The other I/LWEQ module mutants showed similar results (not shown). In addition to using gel filtration and chemical cross-linking we also analyzed mutant L2A using analytical ultracentrifugation. This mutant had an apparent molecular mass of 30 kDa according to sedimentation equilibrium analysis (S. J. Smith and M. G. Fried, unpublished results), which is also consistent with a monomer−dimer equilibrium for this protein, perhaps skewed to the monomer. Taken together, our results demonstrate that the conserved residues of block 4 mediate dimerization of the I/LWEQ module.

Mutation of Block 4 Results in a Decrease in F-Actin Binding Capacity. Actin binding is a critical activity of Talin1 as a component of focal adhesions, and we have previously shown that the I/LWEQ module is likely to contain the primary actin-binding site of Talin1 (*17*). Therefore, we next determined the actin-binding activities of each of the block

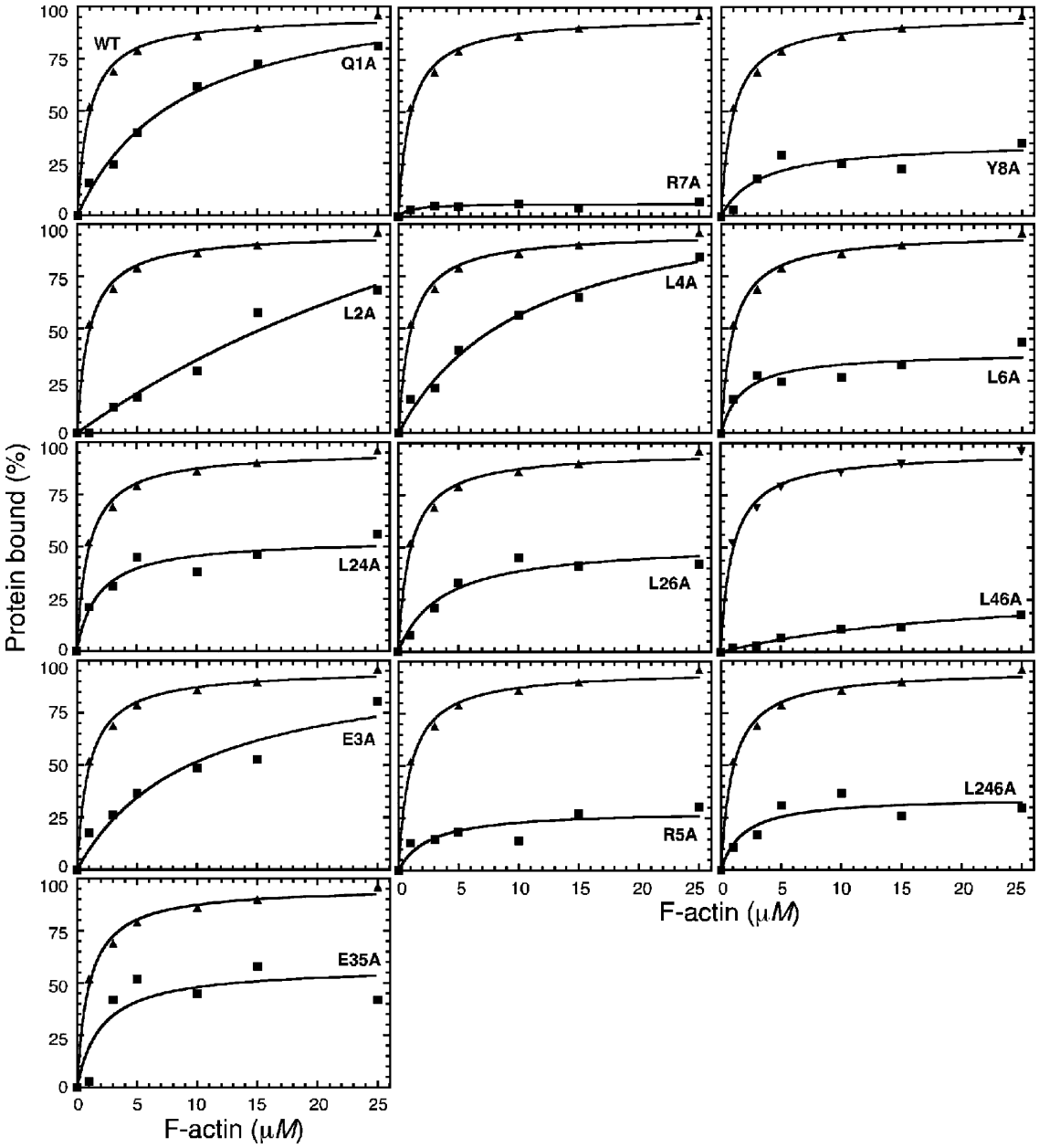

FIGURE 4: F-Actin binding of Talin1 I/LWEQ module mutants. Actin-binding assays were performed for each mutant and plotted with the result for the wild-type protein. The apparent binding affinity for each mutant (single and multiple) was less than for the unmodified protein, as was the total actin-binding capacity (see Table 1). These data are the averages of three to four independent assays for each protein.

4 mutants. In this analysis the dissociation constant of the wild-type I/LWEQ module was 0.97 μM, with a binding capacity of 96%, which is similar to our previous results (*19*). In contrast to the unmodified protein, each of the eight single mutants, four double mutants, and one triple mutant had a reduced actin-binding activity, which is reflected primarily in the reduced maximum binding activity seen with each mutant (Figure 4). For example, the actin-binding activity of R7A was nearly abolished, which is consistent with our previous studies showing that this residue (R2526 of Talin1, R958 of yeast Sla2p) is required for F-actin binding (*17*). The actin-binding capacities of the other mutants were intermediate between wild type and the inactive R7A. These binding data are summarized in Table 1, which shows that the relative association constant for F-actin for each mutant is substantially less than for the Talin1 I/LWEQ module. Our results show that the conserved amino acids of block 4 are required for full actin-binding activity of the Talin1 I/LWEQ module.

I/LWEQ Module Dimerization Has a Role in F-Actin Dynamics. As the link between integrins and the actin cytoskeleton in focal adhesions, both integrin and actin binding are likely to be essential for normal Talin1 function. We have previously shown that the I/LWEQ module of Talin1 both cross-links and stabilizes F-actin against depolymerization (*19*), perhaps due to an ability to bind to the sides of actin filaments. The results presented above indicate that actin binding and dimerization are coupled, and if one formal actin-binding site exists per monomer, then mutants that negatively affect dimerization would be expected to also lessen the F-actin stabilization and cross-linking activities of the Talin1 I/LWEQ module.

In agreement with our previous results, we found that the Talin1 I/LWEQ module inhibited depolymerization of actin

Table 1: Dissociation Constants for F-Actin Binding[a]

I/LWEQ construct	K_d (μM)	relative K_d	B_{max}	R^2
WT	0.97	1.0	96	0.994
Q1A	8.7	9.0	82	0.992
L2A	53	55	68	0.969
E3A	9.6	9.9	74	0.946
L4A	11	11	82	0.986
R5A	2.5	2.6	29	0.787
L6A	1.9	2.0	39	0.963
R7A				
Y8A	3.1	3.2	35	0.858
L24A	1.8	1.9	54	0.936
L26A	3.6	3.7	52	0.956
L46A	22	23	33	0.959
L246A	1.8	1.9	35	0.860
E3R5A	2.0	2.1	58	0.809

[a] Dissociation constants (K_d) for the unmodified (WT) Talin1 and mutant I/LWEQ module constructs were calculated from the data in Figure 4 using GraphPad Prism 4.0 using the expression $Y = B_{max}X/K_d + X$. The R^2 value is for the best fit of the average of three to four independent assays. Comparison of the relative K_d values shows that mutation of the conserved amino acids of block 4 significantly reduces the actin-binding capacity of the Talin1 I/LWEQ module.

filaments when the actin is diluted below the critical concentration for polymerization (Figure 5A). After 10 min, when diluted from 10 to 0.1 μM, F-actin was approximately 42% depolymerized, and the early phase of depolymerization could be readily modeled as a first-order exponential process. When the unmodified Talin1 I/LWEQ module was added as a component of the dilution buffer, the rate of actin depolymerization slowed substantially, and after 10 min, greater than 80% of the F-actin remained, even though the total actin concentration was well below the critical concentration for actin polymerization, which is approximately 0.5 μM under these conditions. When allowed to proceed for longer periods, the actin-only control depolymerized completely, as measured by the decrease in pyrene−actin fluorescence, while the actin + Talin1 I/LWEQ module solution remained stable at greater than 50% F-actin. Each of the block 4 mutants inhibited actin depolymerization but not as well as the wild-type protein (Figure 5). The inhibition activities of the single mutants outside of the putative L2−L6 core (Q1A, R7A, and Y8A) were similar, at 50−55% of the wild type (Figure 5). Our data indicate that mutation of the three leucine residues (L2A, L4A, and L6A) had a progressive effect from the N-terminus to the C-terminus block 4, with the triple mutation (L246A) having a synergistic effect, resulting in a mutant with approximately 35% of the wild-type protein. Mutation of the charged residues (E3A, R5A), individually and together, had the least effect on the inhibition of F-actin depolymerization (Figure 5).

Both Talin1 and the Talin1 I/LWEQ cross-link F-actin filaments into networks and bundles (*17*, *37*). As with the inhibition of actin depolymerization, this activity is likely dependent on the ability of I/LWEQ module dimers to bind simultaneously to two filaments. While we used high-speed sedimentation (160000*g*) to measure actin-binding activity of the I/LWEQ module with increasing actin concentration (Figure 3), we used low-speed sedimentation (13000*g*) of equimolar solutions of F-actin and the I/LWEQ module protein to measure the cross-linking activity of the Talin1 I/LWEQ module and the block 4 mutants. Our results were remarkably similar to those obtained in the F-actin stabilization assay. When F-actin alone was centrifuged at 13000*g*, very little of the protein sedimented (Figure 6, control lane, actin only). Inclusion of the wild-type Talin1 I/LWEQ module resulted in the sedimentation of essentially all of the F-actin (Figure 6, WT lane). The three single mutants (Q1A, R7A, and Y8A) from outside of the putative core of block 4 had activities of 40−60% of wild type. The activities of the single leucine mutants (L2A, L4A, and L6A) and the double mutants L24A and L26A were similar, ranging between 40% and 55%. As with the inhibition of actin polymerization (Figure 5), the triple leucine mutant (L246A) had the largest effect on cross-linking, which was also similar to that of L46A. As with the inhibition of depolymerization, mutation of the charged amino acids E3A and R5A, separately and together, had the least effect on F-actin cross-linking, especially compared to the triple leucine mutation.

The preceding results demonstrated that the I/LWEQ module affects the organization of actin filaments but represent measurements of the bulk properties of filaments under the influence of the Talin1 I/LWEQ module. To examine directly how these proteins affect actin filaments, we used transmission electron microscopy of negatively stained F-actin preparations (Figure 7). As expected, F-actin alone formed a loosely tangled network of ~8 nm filaments on the surface of the grid. When F-actin was mixed with an equimolar amount of the wild-type Talin1 I/LWEQ module, the filaments were markedly more cross-linked. The filaments also formed bundles (Figure 7, actin + WT, arrowheads; see inset). With each mutant the actin filaments were more cross-linked than the actin-only control preparation but did not show the level of cross-linking or evidence of stiff bundles that were observed with the wild-type protein. Thus, while the mutant proteins were apparently capable of cross-linking F-actin, as suggested by the bulk measures of actin organization in solution, they did not have the same effect on actin filaments as the unmodified protein. Taken together, our results demonstrate that dimerization is likely to be essential for the normal interaction between the Talin1 I/LWEQ module and F-actin in cells.

Dimerization and Focal Adhesion Targeting of the Talin1 I/LWEQ Module. In addition to its role as an actin-binding element, we recently showed that the I/LWEQ module is essential for targeting Talin1 to focal adhesions in mammalian cells (*20*). Full-length GFP-Talin1 is targeted to focal adhesions in a variety of cells, but Talin1 lacking the I/LWEQ module does not localize to focal adhesions. A GFP fusion containing only the Talin1 I/LWEQ module is targeted to focal adhesions as well as the full-length protein, which demonstrates that the I/LWEQ module of Talin1 is both necessary and sufficient for focal adhesion targeting. The I/LWEQ modules of other superfamily members, such as those of Sla2p and Hip1, and including Talin2 are not targeted to focal adhesions. Since the amino acids required for dimerization are important for simple F-actin binding and the interaction of the Talin1 I/LWEQ module with actin filaments in vitro (Figures 3−7), we next determined whether these conserved residues are also involved in focal adhesion targeting.

As expected, the unmodified GFP-I/LWEQ module targeted to focal adhesions in HeLa cells plated on fibronectin (Figure 8, row 1, arrowheads). Moreover, most of the fusion protein was found in focal adhesions, as shown by the

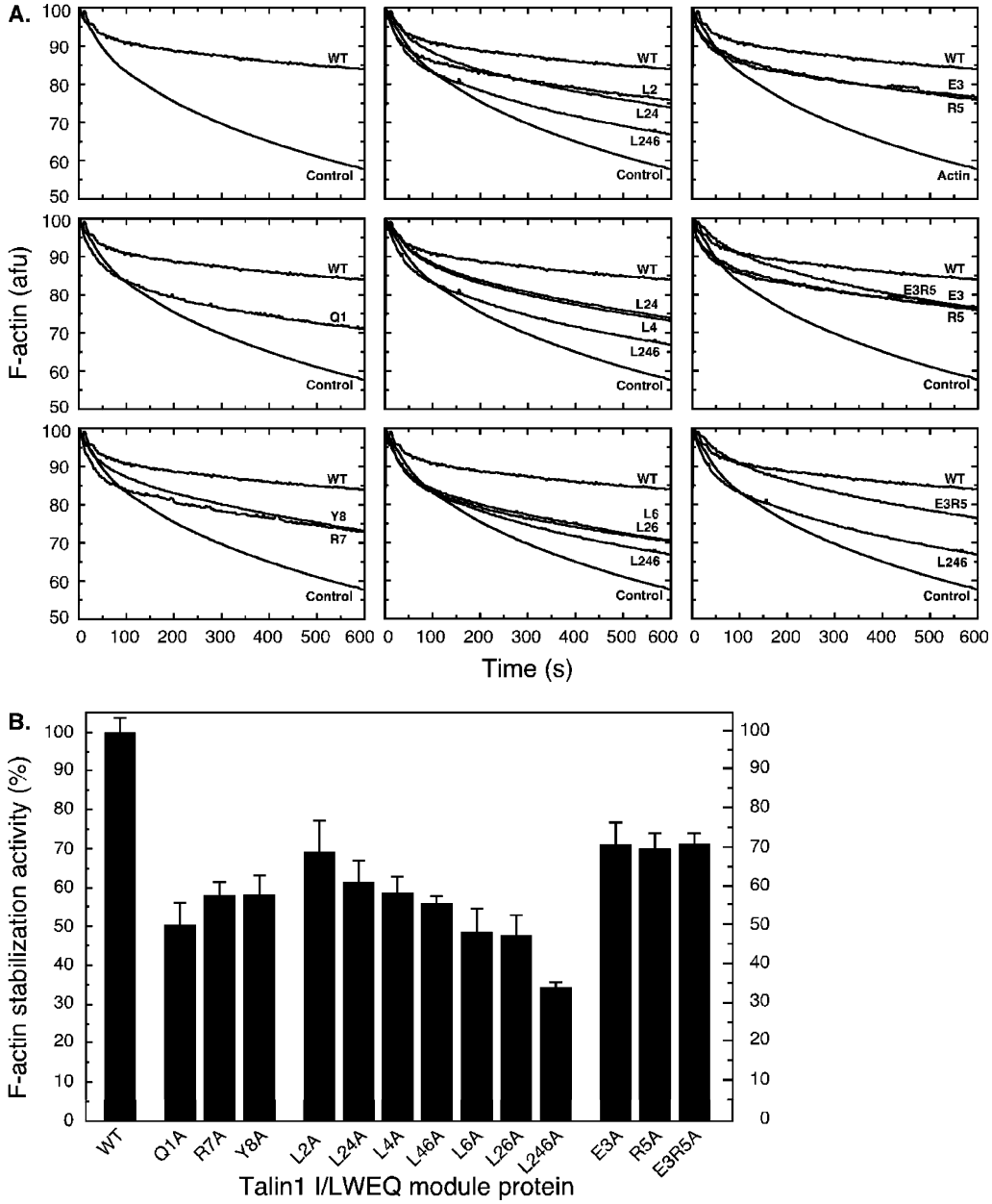

FIGURE 5: F-Actin stabilization against depolymerization. (A) The ability of wild-type and mutant Talin1 I/LWEQ module proteins to stabilize F-actin against depolymerization was assayed for 10 min for each protein. Column 1 includes Q1A, R7A, and Y8A, which are outside of the putative coiled coil core. Column 2 includes the leucine mutants, and column 3 includes the internal E3R5 mutants. Stabilization activity was reduced for each mutant. (B) The data from (A) were normalized to WT stabilization activity = 100% at 10 min. The first group after the WT protein data includes the peripheral mutants (Q1A, R7A, and Y8A). This is followed by the core leucine mutants (L2L4L6) and the core E3R5 mutants. The triple L246A mutant had the greatest effect on stabilization activity, while the E3R5 single and double mutants had the lowest effects. Data are the mean + SD for three to five independent assays.

yellow/yellow-green color of the overlay of the vinculin (red) and GFP-Talin1 (green) channels, with very little exogenous GFP-Talin1 I/LWEQ evident in the cytoplasm outside of focal adhesions. The Q1A, E3A, and R5A mutants (Figure 8, row 2, arrowheads) were also targeted to focal adhesions. The L2A mutant targeted well to focal adhesions (Figure 8, row 3, arrowhead). We observed slight evidence of targeting with L4A and L24A, but both of these mutants also had significant diffuse GFP-fusion protein in the cytoplasm. The R7A mutant did not target to focal adhesions, which is shown by the complete absence of GFP-Talin1 I/LWEQ module colocalization with vinculin in the merged image (Figure 8, row 4, red focal adhesions, arrowheads). This is in agreement with our previous study of Talin1 focal adhesion targeting, where we found that this mutant neither binds to F-actin with high capacity nor targets to focal adhesions (*20*). None of the mutants containing L6A (L6A, L26A, L46A, L246A) targeted to focal adhesions (Figure 8, rows 4 and 5, red channel only visible in the merged image, arrowheads). In general, the leucine mutants also showed relatively low levels of chemical cross-linking (Figure 3B); F-actin stabilization activity, especially in the context of the triple leucine mutation (Figure 5B); and cross-linking activity, as assayed by low-speed sedimentation (Figure 6). These results are consistent with our hypothesis that dimerization is linked to the biological functions of Talin1, including focal adhesion targeting. In contrast to the leucine multiple mutants, the E3R5A double mutant showed a low level of focal adhesion

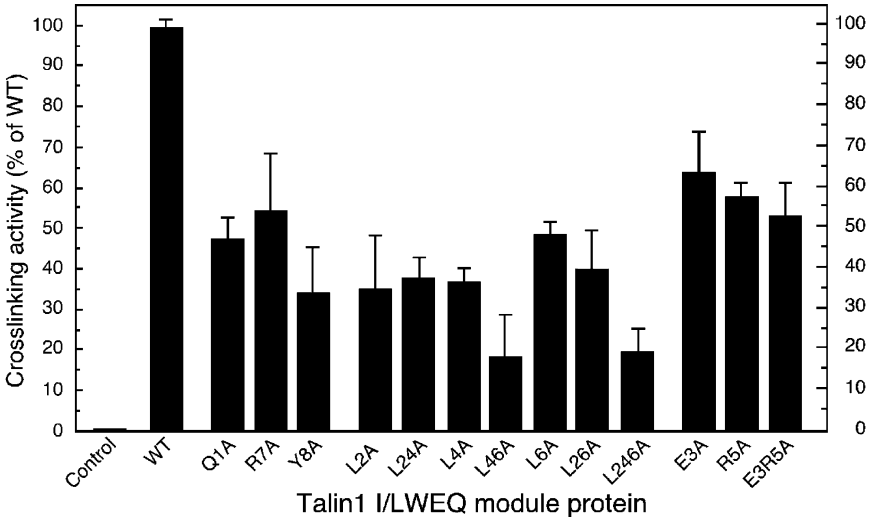

FIGURE 6: Cross-linking of actin filaments by the Talin1 I/LWEQ module. Low-speed sedimentation was used to determine the ability of the Q1-Y8 mutants to cross-link actin filaments. The data were normalized using WT = 100% cross-linking activity. These results are similar to the F-actin stabilization data (Figure 5). The L46A and L246A mutants had the lowest capacities to cross-link actin filaments, perhaps due to its higher monomeric character than the other mutants and the wild-type protein. The control is F-actin alone, which did not sediment at 13000*g*. Data are the mean + SD of four to five independent assays.

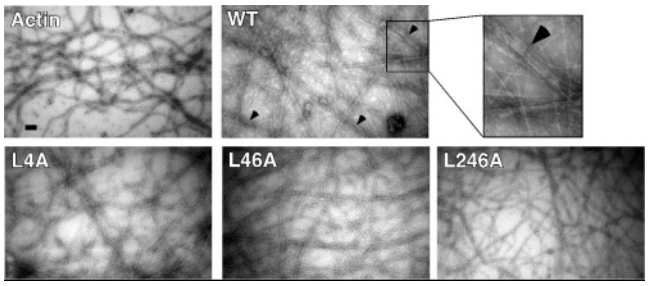

FIGURE 7: Cross-linking and bundling of individual actin filaments by the Talin1 I/LWEQ module. Transmission electron microscopy revealed that the wild-type Talin1 I/LWEQ module cross-linked bundled F-actin into a stiff network of cross-linked filaments that also contained bundles of 8−10 filaments (top row, center, and inset, arrowheads). Three representative leucine mutants (L4A, L26A, and L246A) are shown in row 2. None of these mutants was capable of inducing F-actin bundle formation, and the cross-linked networks in the presence of the mutant proteins were not as extensive as for the wild-type protein. Similar results were obtained with the other mutants (not shown).

targeting (Figure 8, row 5), which is consistent with the less severe phenotype of this mutant compared to that of the multiple leucine mutations (cf. Figures 5 and 6).

DISCUSSION

Our long-term goal is to understand how members of the I/LWEQ module protein superfamily function as linkers to the actin cytoskeleton as components of multiprotein assemblies (*19*−*21*, *38*). In this report we have focused on Talin1. Previous studies from a number of different laboratories have shown that Talin1 is a critical component of focal adhesions. For example, Talin1 is required for the assembly of focal adhesion complexes (*6*, *39*) and the establishment of the mechanical link between the actin cytoskeleton and the ECM that is required for cell adhesion and cell motility (*27*). These properties are due to the capacity of Talin1 to bind to both F-actin and the cytoplasmic tail of β-integrin. Talin1 is also essential for integrin activation (*40*−*42*). These different functions of Talin1 are due to its modular structure. The N-terminal FERM domain is involved in integrin activation, while the central α-helical rod domain contains at least three sites for interaction with the focal adhesion component vinculin (*43*). The C-terminal I/LWEQ module specifies F-actin binding (*17*), and we have also recently shown that this conserved element is both necessary and sufficient for targeting Talin1 to focal adhesions (*20*). Previous studies have shown that Talin1 exists as a dimer (*30*), but the functional significance of dimerization has not been addressed directly.

In this report we have shown that the C-terminus of the I/LWEQ module of Talin1 contains a dimerization determinant coextensive with an α-helix that is predicted to form a coiled coil stabilized by hydrophobic interactions between three conserved leucine residues and two electrostatic interactions between a conserved glutamic acid and arginine (Figure 9). Our results support this model. Alanine-scanning mutagenesis of the residues predicted to form the core of the coiled coil and the adjacent conserved amino acids on the same face of the putative block 4 α-helix/coiled coil produced proteins that are less dimeric than the wild-type protein. Moreover, these mutations affect properties of the Talin1 I/LWEQ module that are likely to be important for the function of Talin1 in focal adhesion complexes. Our results show that these mutants have decreased actin-binding capacity, which is reflected by a decrease both in the apparent association constants for F-actin and in the maximal binding capacity for F-actin. These defects are generally more pronounced in the latter. These block 4 mutants also have lower F-actin cross-linking activity and lower F-actin stabilization activity than the wild type protein, which are likely to be due to both a lower affinity/capacity for F-actin binding and a decrease in dimeric character.

In addition to these effects on F-actin interactions, mutation of these conserved amino acids also affects focal adhesion targeting of the Talin1 I/LWEQ module (Table 2). As expected from our previous studies (*17*), we confirmed that the conserved arginine-2526 is required for actin binding and for focal adhesion targeting. This R7A mutant neither bound to F-actin nor targeted to focal adhesions. However, the

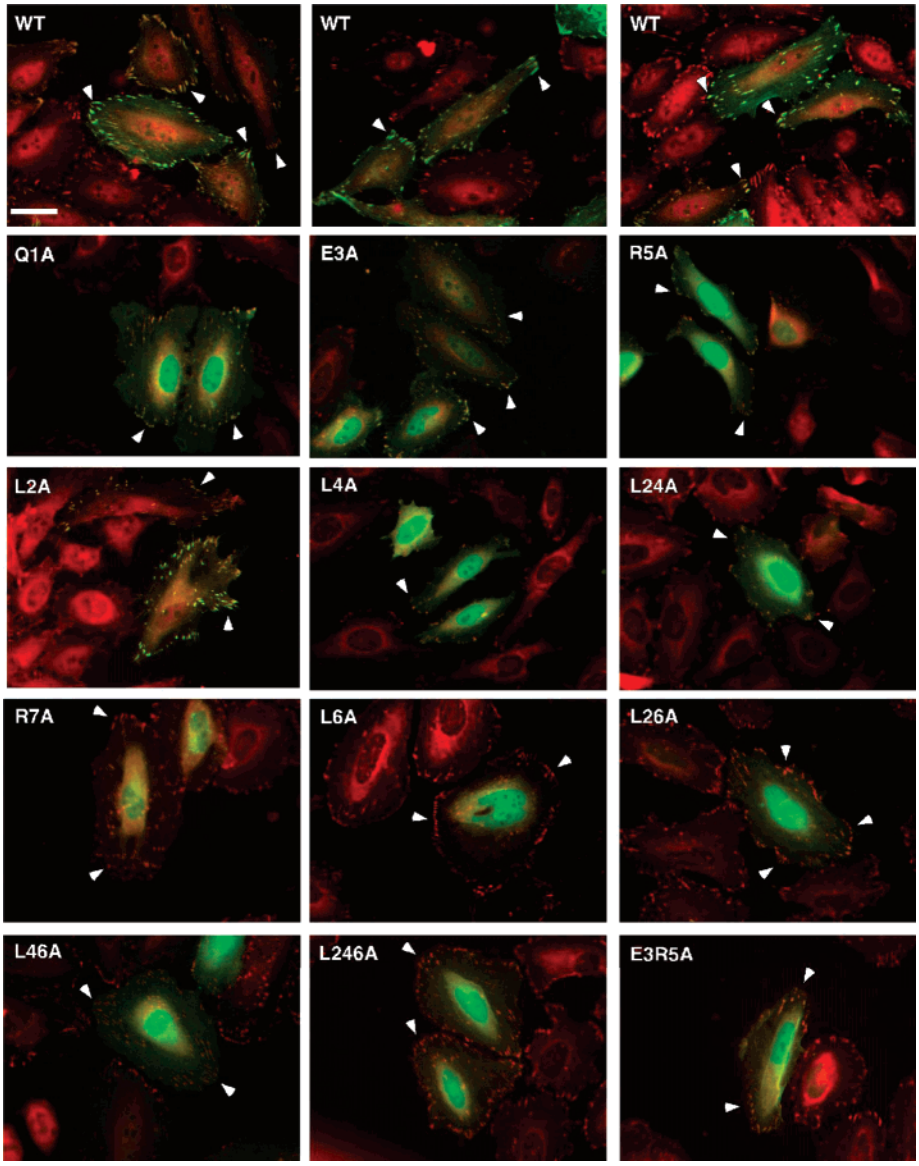

FIGURE 8: Focal adhesion targeting of the Talin1 I/LWEQ module. HeLa cells plated on fibronectin were transiently transfected with each of the wild-type (row 1) or single, double, and triple alanine mutant I/LWEQ module construct (rows 2−5). Representative image overlays of the GFP-Talin1 I/LWEQ module (green) and vinculin (red) demonstrate that the Talin1 I/LWEQ module colocalizes with vinculin in focal adhesion complexes, while mutant I/LWEQ module proteins generally colocalize less with vinculin at focal adhesion complexes. L6A and the multiple leucine mutants containing L6A were not targeted to focal adhesions (no merge of GFP-Talin1 I/LWEQ and vinculin signal). These data are summarized in Table 2.

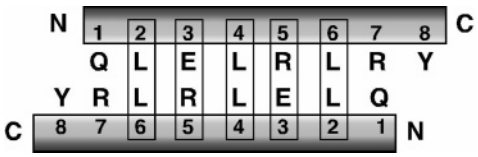

FIGURE 9: Block 4 dimer. Our data support this model, in which the three leucine pairs (L2−L6, L4−L4, and L6−L2) and the two E3−R5 pairs mediate dimerization of block 4. The internal charged residues are hypothesized to specify the putative antiparallel nature of the coiled coil.

conserved R7K mutant is targeted to focal adhesions despite having little actin-binding activity (*20*). We do not yet understand why a positively charged amino acid at this position is sufficient for focal adhesion targeting but not actin binding. This result does indicate that actin binding and focal adhesion targeting are not directly coupled in Talin1. In contrast to R7A, mutant Q1A, which is also outside of the coiled coil core, targeted to focal adhesions but not as well as the wild-type protein. These data, along with observation that the L6A mutant did not colocalize with vinculin in focal

Table 2: Focal Adhesion Targeting[a]

Talin1 construct	FAT	Talin1 construct	FAT
full length	+++++	R7A	−
I/LWEQ	+++++	Y8A	+
Q1A	++++	L24A	+
L2A	++++	L26A	−
E3A	++	L46A	−
L4A	++	L246A	−
R5A	++	E3R5A	+
L6A	−		

[a] We showed previously that full-length Talin1 and the Talin1 I/LWEQ module are targeted equally well to focal adhesions (*20*). In this report we have found that the block 4 I/LWEQ module mutants target less well to focal adhesions in HeLa cells (Figure 8). Mutant L6A and the multiple leucine mutants containing this mutation were not targeted to focal adhesions. FAT: focal adhesion targeting.

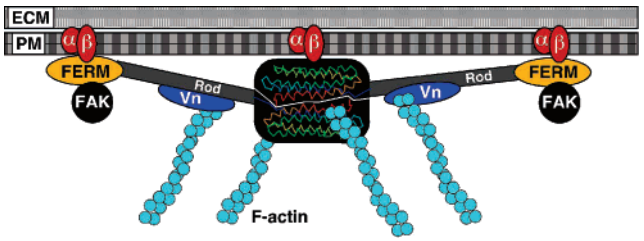

FIGURE 10: Model of the full-length Talin1 dimer. The results presented here and our previous studies on focal adhesion targeting and actin binding of Talin1 indicate that the primary dimerization motif in Talin1 is at the C-terminus of the I/LWEQ module (block 4 α-helices in red-orange). The I/LWEQ module dimer also contains an essential focal adhesion targeting signal, which is abolished in mutants that have substantial monomeric character (e.g., L246A). A C-terminal integrin-binding site may account for this focal adhesion targeting. Our results also indicate that the C-terminus of the I/LWEQ module is likely to contain a primary F-actin binding site for Talin1 and that dimerization is necessary for full actin binding. Key: FERM, N-terminal Talin1 FERM domain; Rod, rod domain which consists of conserved α-helical repeats; FAK, focal adhesion kinase; Vn, vinculin; α/*β*, integrins; ECM, extracellular matrix; PM, plasma membrane. The five-helix bundle of the I/LWEQ module is based on our previous prediction (*19*) and is similar to the structure of the Hip1 I/LWEQ module, which lacks the final block 4 α-helix, which is shown in red (*29*).

adhesions, indicate that the C-terminus of block 4 is more important for subcellular targeting than the N-terminus. The subcellular localization of the multiple L26A, L46A, and L246A mutants, which were not targeted to focal adhesions, also supports this conclusion. The behavior of these mutants also indicates that the conserved leucine residues are more important for targeting than the other residues, including the E3R5 glutamate−arginine pair. Although the E3R5 mutants, together and separately, were similarly defective in actin binding, they were generally less defective in actin cross-linking and stabilization than the multiple leucine mutants. Mutant Y8A, which is outside of the core and retains substantial dimeric character, is nevertheless defective in each of the other properties examined in this work. Further studies complementary to those presented here will be required to fully understand the role of this conserved residue. A detailed comparison of *Drosophila* talin and mammalian Talin1 may reveal the importance of Y8. *Drosophila* talin has a single insertion the removes Y8 from the conserved face of the block 4 α-helix (*21*). It has been shown that subcellular targeting of this talin I/LWEQ module to integrin-based adhesion sites requires endogenous talin (*9*, *44*). It will be interesting to determine how actin binding and stabilization are different with this talin compared to the other I/LWEQ modules.

It has long been known that Talin1 is a dimer when purified from native sources such as platelets, and the available data suggest that Talin1 exists as an antiparallel dumbbell-shaped dimer (*30*). On the basis of the data presented here, we propose that the block 4 dimerization motif is responsible for Talin1 dimerization, with the central I/LWEQ module dimer targeting the protein to focal adhesions, while the FERM domains extend out from the I/LWEQ module dimer in opposite directions (Figure 10). This conformation is similar to that of filamin, which, like Talin1, is a large, modular cytoskeletal protein found at the plasma membrane (*45*). Taken together, our results indicate that dimerization mediated by the conserved amino acids of block 4 is essential for normal Talin1 function. Further research will be required to identify the exact mechanism of dimerization. In preliminary experiments we have found that a chemically synthesized peptide consisting only of the amino acids of block 4 of Talin1 forms a very stable α-helical dimer, which is disrupted only by lengthy incubation at 100 °C or in the presence of 8 M urea (S. J. Smith and R. O. McCann, unpublished results). Thus, the block 4 dimerization motif is likely to be strong enough for the maintenance of a stable dimer in vivo. We are currently characterizing how mutation of the putative coiled coil core amino acids affects peptide dimer stability and orientation. These studies and further analysis of a three-dimensional structure of the I/LWEQ module that includes block 4 [cf. the THATCH/LATCH structure of Hip1R (*29*)] will elucidate how these proteins interact with their partners.

At the other end of the spectrum, it will be necessary to analyze the behavior of these mutants in the context of the full-length protein. Although we have previously shown that several critical functions, including actin binding and focal adhesion targeting of mammalian Talin1 and the *Ciona intestinalis* Talin-a alternative splice variant, are properties of the I/LWEQ module (*38*), incorporation of these mutants, as well as the truncation mutants (Figure 1), into the full-length protein will allow us to determine how dimerization, actin−Talin1 interactions, and focal adhesion targeting are coupled in focal adhesions in cells. For example, recent research on the dynamics of different classes of focal adhesion proteins has led to the attractive hypothesis that actin-binding proteins such as Talin1 act as a molecular clutch for cell motility in focal adhesions (*32*). The actin-binding, dimerization, and focal adhesion targeting mutants of Talin1 described here will provide new constructs to further test this hypothesis. Other I/LWEQ module elements, including the highly charged opposite face of the block 4 α-helix, are also candidates for mutagenesis. We are currently analyzing their actin-binding and subcellular targeting properties.

Finally, block 4 is highly conserved in other I/LWEQ module proteins, including talins from amoebozoans such as *Dictyostelium discoideum* and *Entamoeba histolytica*. The roles of *D. discoideum* TalA and TalB have been studied (*46*−*49*). In the case of *E. histolytica*, which is responsible for as many as 50000 annual deaths worldwide due to amoebiasis and amoebic dysentery, cell adhesion and cell motility are virulence factors in *Entamoeba* infections. Therefore, the study of *E. histolytica* talin as a component of the adhesion plate, which is structurally analogous to the focal adhesion complex in animal cells, may lead to a better understanding of *Entamoeba* pathogenesis (*50*, *51*). We have recently shown that Talin2, which is not a focal adhesion component, is induced during striated muscle differentiation and is a component of stable adhesion complexes such as costameres and intercalated disks (*52*). We expect that our results on Talin1 will provide a foundation for the study of Talin2 in muscle assembly. Similarly, we anticipate that the use of cognate block 4 mutations in the study of Sla2p and Hip1/Hip1R/Hip12 will lead to a deeper understanding of the roles of these I/LWEQ module proteins in endocytosis and vesicle trafficking (*24*, *53*, *54*).

ACKNOWLEDGMENT

We thank Melissa A. Senetar and Stanley J. Foster for help with early work on the dimerization of the I/LWEQ module, Mary Gail Engle of the University of Kentucky Electron Microscopy and Imaging Facility for help with the electron microscopy, Michael G. Fried for help with analytical ultracentrifugation, and Richard H. Singiser for reading the manuscript.

REFERENCES

1. Critchley, D. R. (2000) Focal adhesions—the cytoskeletal connection, *Curr. Opin. Cell Biol. 12*, 133−139.
2. Lo, S. H. (2006) Focal adhesions: what's new inside, *Dev. Biol. 294*, 280−291.
3. Burridge, K., and Connell, L. (1983) A new protein of adhesion plaques and ruffling membranes, *J. Cell Biol. 97*, 359−367.
4. Burridge, K., and Connell, L. (1983) Talin: a cytoskeletal component concentrated in adhesion plaques and other sites of actin-membrane interaction, *Cell Motil. 3*, 405−417.
5. Horwitz, A., Duggan, K., Buck, C., Beckerle, M. C., and Burridge, K. (1986) Interaction of plasma membrane fibronectin receptor with talin—a transmembrane linkage, *Nature 320*, 531−533.
6. Priddle, H., Hemmings, L., Monkley, S., Woods, A., Patel, B., Sutton, D., Dunn, G. A., Zicha, D., and Critchley, D. R. (1998) Disruption of the talin gene compromises focal adhesion assembly in undifferentiated but not differentiated embryonic stem cells, *J. Cell Biol. 142*, 1121−1133.
7. Chishti, A. H., Kim, A. C., Marfatia, S. M., Lutchman, M., Hanspal, M., Jindal, H., Liu, S. C., Low, P. S., Rouleau, G. A., Mohandas, N., Chasis, J. A., Conboy, J. G., Gascard, P., Takakuwa, Y., Huang, S. C., Benz, E. J., Jr., Bretscher, A., Fehon, R. G., Gusella, J. F., Ramesh, V., Solomon, F., Marchesi, V. T., Tsukita, S., Tsukita, S., Arpin, M., Louvard, D., Tonks, N. K., Anderson, J. M., Fanning, A. S., Bryant, P. J., Woods, D. F., and Hoover, K. B. (1998) The FERM domain: a unique module involved in the linkage of cytoplasmic proteins to the membrane, *Trends Biochem. Sci. 23*, 281−282.
8. Calderwood, D. A., and Ginsberg, M. H. (2003) Talin forges the links between integrins and actin, *Nat. Cell Biol. 5*, 694−697.
9. Tanentzapf, G., and Brown, N. H. (2006) An interaction between integrin and the talin FERM domain mediates integrin activation but not linkage to the cytoskeleton, *Nat. Cell Biol. 8*, 601−606.
10. Parsons, J. T., Martin, K. H., Slack, J. K., Taylor, J. M., and Weed, S. A. (2000) Focal adhesion kinase: a regulator of focal adhesion dynamics and cell movement, *Oncogene 19*, 5606−5613.
11. Di Paolo, G., Pellegrini, L., Letinic, K., Cestra, G., Zoncu, R., Voronov, S., Chang, S., Guo, J., Wenk, M. R., and De Camilli, P. (2002) Recruitment and regulation of phosphatidylinositol phosphate kinase type 1γ by the FERM domain of talin, *Nature 420*, 85−89.
12. Hemmings, L., Rees, D. J., Ohanian, V., Bolton, S. J., Gilmore, A. P., Patel, B., Priddle, H., Trevithick, J. E., Hynes, R. O., and Critchley, D. R. (1996) Talin contains three actin-binding sites each of which is adjacent to a vinculin-binding site, *J. Cell Sci. 109*, 2715−2726.
13. Borowsky, M. L., and Hynes, R. O. (1998) Layilin, a novel talin-binding transmembrane protein homologous with C-type lectins, is localized in membrane ruffles, *J. Cell Biol. 143*, 429−442.
14. Johnson, R. P., and Craig, S. W. (1994) An intramolecular association between the head and tail domains of vinculin modulates talin binding, *J. Biol. Chem. 269*, 12611−12619.
15. Tremuth, L., Kreis, S., Melchior, C., Hoebeke, J., Ronde, P., Plancon, S., Takeda, K., and Kieffer, N. (2004) A fluorescence cell biology approach to map the second integrin-binding site of talin to a 130 amino acid sequence with the rod domain, *J. Biol. Chem. 279*, 22258−22266.
16. Coutts, A., MacKenzie, E., Griffith, E., and Black, D. (2003) TES is a novel focal adhesion protein with a role in cell spreading, *J. Cell Sci. 116*, 897−906.
17. McCann, R. O., and Craig, S. W. (1997) The I/LWEQ module: a conserved sequence that signifies F-actin binding in functionally diverse proteins from yeast to mammals, *Proc. Natl. Acad. Sci. U.S.A. 94*, 5679−5684.
18. McCann, R. O., and Craig, S. W. (1999) Functional genomic analysis reveals the utility of the I/LWEQ module as a predictor of protein:actin interaction, *Biochem. Biophys. Res. Commun. 266*, 135−140.
19. Senetar, M. A., Foster, S. J., and McCann, R. O. (2004) Intrasteric inhibition mediates the interaction of the I/LWEQ module proteins Talin1, Talin2, Hip1, and Hip12 with actin, *Biochemistry 43*, 15418−15428.
20. Franco, S. J., Senetar, M. A., Simonson, W., Huttenlocher, A., and McCann, R. O. (2006) The conserved C-terminal I/LWEQ module targets Talin1 to focal adhesions, *Cell Motil. Cytoskeleton 63*, 563−581.
21. Senetar, M. A., and McCann, R. O. (2005) Gene duplication and functional divergence during evolution of the cytoskeletal linker protein talin, *Gene 362*, 141−152.
22. Stahelin, R. V., Long, F., Peter, B. J., Murray, D., De Camilli, P., McMahon, H. T., and Cho, W. (2003) Contrasting membrane interaction mechanisms of AP180 N-terminal homology (ANTH) and epsin N-terminal homology (ENTH) domains, *J. Biol. Chem. 278*, 28993−28999.
23. Castagnetti, S., Behrens, R., and Nurse, P. (2005) End4/Sla2 is involved in establishment of a new growth zone in *Schizosaccharomyces pombe*, *J. Cell Sci. 118*, 1843−1850.
24. Baggett, J. J., D'Aquion, K. E., and Wendland, B. (2003) The Sla2p Talin domain plays a role in endocytosis in *Saccharomyces cerevisiae*, *Genetics 165*, 1661−1674.
25. Kaksonen, M., Sun, Y., and Drubin, D. G. (2003) A pathway for association of receptors, adaptors, and actin during endocytic internalization, *Cell 115*, 475−487.
26. Engqvist-Goldstein, A. E., Kessels, M. M., Chopra, V. S., Hayden, M. R., and Drubin, D. G. (1999) An actin-binding protein of the Sla2/Huntingtin interacting protein-1 family is a novel component of clathrin-coated pits and vesicles, *J. Cell Biol. 147*, 1503−1518.
27. Jiang, G., Giannone, G., Critchley, D. R., Fukumoto, E., and Sheetz, M. P. (2003) Two-piconewton slip bond between fibronectin and the cytoskeleton depends on talin, *Nature 424*, 334−337.
28. Monkley, S. J., Zhou, X. H., Kinston, S. J., Giblett, S. M., Hemmings, L., Brown, J. E., Pritchard, C. A., Critchley, D. R., and Fassler, R. (2000) Disruption of the talin gene arrests mouse development at the gastrulation stage, *Dev. Dyn. 219*, 560−574.
29. Brett, T. J., Legendre-Guillemin, V., McPherson, P. S., and Fremont, D. H. (2006) Structural definition of the F-actin-binding THATCH domain from HIP1R, *Nat. Struct. Mol. Biol. 13*, 121−130.
30. Goldmann, W. H., Bremer, A., Haner, M., Aebi, U., and Isenberg, G. (1994) Native talin is a dumbbell-shaped homodimer when it interacts with actin, *J. Struct. Biol. 112*, 3−10.
31. Lupas, A., Van Dyke, M., and Stock, J. (1991) Predicting coiled coils from protein sequences, *Science 252*, 1162−1164.
32. Hu, K., Ji, L., Applegate, K. T., Danuser, G., and Waterman-Storer, C. M. (2007) Differential transmission of actin motion within focal adhesions, *Science 315*, 111−115.
33. Cooper, J. A., Walker, S. B., and Pollard, T. D. (1983) Pyrene actin: documentation of the validity of a sensitive assay for actin polymerization, *J. Muscle Res. Cell Motil. 4*, 253−262.
34. Berger, B., Wilson, D. B., Wolf, E., Tonchev, T., Milla, M., and Kim, P. S. (1995) Predicting coiled coils by use of pairwise residue correlations, *Proc. Natl. Acad. Sci. U.S.A. 92*, 8259−8263.
35. Lupas, A. N., and Gruber, M. (2005) The structure of alpha-helical coiled coils, *Adv. Protein Chem. 70*, 37−78.
36. McClain, D. L., Gurnon, D. G., and Oakley, M. G. (2002) Importance of potential interhelical salt-bridges involving interior residues for coiled coil stability and quaternary structure, *J. Mol. Biol. 324*, 257−270.
37. Schmidt, J. M., Zhang, J., Lee, H. S., Stromer, M. H., and Robson, R. M. (1999) Interaction of talin with actin: sensitive modulation of filament crosslinking activity, *Arch. Biochem. Biophys. 366*, 139−150.
38. Singiser, R. H., and McCann, R. O. (2006) Evidence that talin alternative splice variants from *Ciona intestinalis* have different roles in cell adhesion. *BMC Cell Biol. 7*, 40.
39. Albiges-Rizo, C., Frachet, P., and Block, M. R. (1995) Down regulation of talin alters cell adhesion and the processing of the alpha 5 beta 1 integrin, *J. Cell Sci. 108*, 3317−3329.
40. Calderwood, D. A. (2004) Integrin activation, *J. Cell Sci. 117*, 657−666.

41. Cram, E. J., and Schwarzbauer, J. (2004) The talin wags the dog: new insights into integrin activation, *Trends Cell Biol. 14*, 55−57.
42. Ratnikov, B. I., Partridge, A. W., and Ginsberg, M. H. (2005) Integrin activation by talin, *J. Thromb. Haemostasis 3*, 1783−1790.
43. Gingras, A. R., Ziegler, W. H., Frank, R., Barsukov, I. L., Roberts, G. C., Critchley, D. R., and Emsley, J. (2005) Mapping and consensus sequence identification for multiple vinculin binding sites within the talin rod, *J. Biol. Chem. 280*, 37217−37224.
44. Tanentzapf, G., Martin-Bermudo, M. D., Hicks, M. S., and Brown, N. H. (2006) Multiple factors contribute to integrin-talin interactions in vivo, *J. Cell Sci. 119*, 1632−1644.
45. Feng, Y., and Walsh, C. A. (2004) The many faces of filamin: A versatile molecular scaffold for cell motility and signalling, *Nat. Cell Biol. 6*, 1034−1038.
46. Tsujioka, M., Machesky, L. M., Cole, S. L., Yahata, K., and Inouye, K. (1999) A unique talin homologue with a villin headpiece-like domain is required for multicellular morphogenesis in *Dictyostelium*, *Curr. Biol. 9*, 389−392.
47. Niewohner, J., Weber, I., Maniak, M., Muller-Taubenberger, A., and Gerisch, G. (1997) Talin-null cells of *Dictyostelium* are strongly defective in adhesion to particle and substrate surfaces and slightly impaired in cytokinesis, *J. Cell Biol. 138*, 349−361.
48. Kreitmeier, M., Gerisch, G., Heizer, C., and Muller-Taubenberger, A. (1995) A talin homologue of *Dictyostelium* rapidly assembles at the leading edge of cells in response to chemoattractant, *J. Cell Biol. 129*, 179−188.
49. Tsujioka, M., Yoshida, K., and Inouye, K. (2004) Talin B is required for force transmission in morphogenesis of *Dictyostelium*, *EMBO J. 23*, 2216−2225.
50. Vazquez, J., Franco, E., Reyes, G., and Meza, I. (1995) Characterization of adhesion plates induced by the interaction of *Entamoeba histolytica* trophozoites with fibronectin, *Cell Motil. Cytoskeleton 32*, 37−45.
51. Ackers, J. P., and Mirelman, D. (2006) Progress in research on *Entamoeba histolytica* pathogenesis, *Curr. Opin. Microbiol. 9*, 367−373.
52. Senetar, M. A., Moncman, C. L., and McCann, R. O. (2007) Talin2 is induced during striated muscle differentiation and is targeted to stable adhesion complexes in mature muscle, *Cell Motil. Cytoskeleton 64*, 157−173.
53. Gourlay, C. W., Dewar, H., Warren, D. T., Costa, R., Satish, N., and Ayscough, K. R. (2003) An interaction between Sla1p and Sla2p plays a role in regulating actin dynamics and endocytosis in budding yeast, *J. Cell Sci. 116*, 2551−2564.
54. Metzler, M., Legendre-Guillemin, V., Gan, L., Chopra, V., Kwok, A., McPherson, P. S., and Hayden, M. R. (2001) HIP1 functions in clathrin-mediated endocytosis through binding to clathrin and adaptor protein 2, *J. Biol. Chem. 276*, 39271−39276.

BI700637A